Available online at www.sciencedirect.com

ScienceDirect

Journal of the Chinese Medical Association 81 (2018) 170−177

www.jcma-online.com

Original Article

Abnormal biventricular performance in asymptomatic adolescents late after repaired Tetralogy of Fallot: Combined two-dimensional speckle tracking and three-dimensional echocardiography study

Ken-Pen Weng [a,b,c,*], Yu-Chi Hung [d], Shih-Hui Huang [e], Huang-Wei Wu [f], Kuang-Jen Chien [a], Chu-Chuan Lin [a], Hsu-Hsia Peng [g], Ming-Ting Wu [h]

[a] *Department of Pediatrics, Kaohsiung Veterans General Hospital, Kaohsiung, Taiwan, ROC*
[b] *Faculty of Medicine, School of Medicine, National Yang Ming University, Taipei, Taiwan, ROC*
[c] *Shu-Zen College of Medicine and Management, Kaohsiung, Taiwan, ROC*
[d] *Department of Pediatrics, St. Joseph Hospital, Kaohsiung, Taiwan, ROC*
[e] *Department of Nursing, Fooyin University, Kaohsiung, Taiwan, ROC*
[f] *Department of Pediatrics, Kaohsiung Armed Forces General Hospital, Kaohsiung, Taiwan, ROC*
[g] *Department of Biomedical Engineering and Environmental Sciences, National Tsing Hua University, Hsinchu, Taiwan, ROC*
[h] *Department of Radiology, Kaohsiung Veterans General Hospital, Kaohsiung, Taiwan, ROC*

Received March 21, 2017; accepted September 1, 2017

Abstract

Background: The aim of this prospective study was to assess biventricular performance in asymptomatic adolescents with repaired tetralogy of Fallot (TOF) using 2D speckle tracking and real time 3D echocardiography simultaneously.
Methods: We studied 31 patients with repaired TOF (M/F: 22/9, age: 16.1 ± 6.1 yrs) who had history of cardiac surgery with mean follow-up duration of 12.8 years, and 32 age- and sex-matched normal individuals (M/F: 23/9, age: 16.6 ± 5.1 yrs). All subjects underwent speckle tracking and 3D echocardiography, electrocardiogram, treadmill, and blood sampling for measurement of brain natriuretic peptide (BNP).
Results: Compared to the control group, the TOF group had higher BNP level (31.8 ± 21.4 vs 14.1 ± 12.4 pg/ml, $p < 0.01$), lower peak oxygen consumption (8.4 ± 1.7 vs 9.9 ± 1.6 ml/kg/min, $p < 0.05$), and longer QRS duration (126 ± 30 vs 82 ± 9 ms, $p < 0.01$). Patients with repaired TOF had significantly impaired right ventricle (RV) global and all six regional longitudinal strain and strain rate than normal controls. Left ventricle (LV) global and mainly apical regional longitudinal strain and strain rate were reduced in patients with repaired TOF. There was a significant correlation of global longitudinal strain (r = 0.456, $p = 0.01$) and global time to peak longitudinal strain (r = 0.484, $p < 0.01$) between LV and RV in patients with repaired TOF. In terms of 3D echo cardiographic volume data, patients with repaired TOF had lower LV stroke volume index ($p < 0.05$), but higher RV end diastolic volume index ($p < 0.01$), RV end systolic volume index ($p < 0.01$), RV stroke volume index ($p < 0.01$), and pulmonary regurgitation fraction ($p < 0.01$) than normal controls.
Conclusion: Our results suggest asymptomatic adolescents with repaired TOF had abnormal biventricular myocardial performance, as demonstrated by combined 2D speckle-tracking and 3D echocardiography. The implications of these findings for management of adolescents late after repaired TOF remain to be determined.

Keywords: 2D speckle tracking echocardiography; Real time 3D echocardiography; Strain; Strain rate; Tetralogy of Fallot

Conflicts of interest: The authors declare that they have no conflicts of interest related to the subject matter or materials discussed in this article.

* Corresponding author. Dr. Ken-Pen Weng, Department of Pediatrics, Kaohsiung Veterans General Hospital, 386, Ta-Chung 1st Road, Kaohsiung 813, Taiwan, ROC.
E-mail address: kenpenweng@yahoo.com.tw (K.-P. Weng).

https://doi.org/10.1016/j.jcma.2017.09.012

1. Introduction

Tetralogy of Fallot (TOF) is the most common cyanotic congenital heart disease and is more highly prevalent in Taiwan (0.62/1000) than that in western reports (0.26−0.47/1000).[1] With the advances of intracardiac surgery, the prognosis of TOF has improved greatly and the 30-year survival rate is estimated to be >90%.[2] However, a variable degree of pulmonary regurgitation (PR) may develop later after repair of TOF. It may lead to right ventricle (RV) volume overload and dysfunction, exercise intolerance, and development of potentially life threatening arrhythmias.[3−5] In addition, the presence of left ventricle (LV) dysfunction related to PR and RV dilation in patients with repaired TOF has been demonstrated in the previous studies.[6−9] The ventricular interaction may be related to shared myocardial fibers, electromechanical asynchrony, or a geometrical interaction with septal shift in the limited pericardial sac.[10−12]

Recent studies showed that LV dysfunction is associated with death and life threatening ventricular arrhythmias.[3,7] Biventricular impairment is important to assess in asymptomatic patients with repaired TOF because of its high likelihood of occurrence.

Two-dimensional (2D) speckle tracking echocardiography (STE) is not angle dependent and not affected by tethering effects. It has been proved to identify biventricular impairment early in patients with repaired TOF, and can be combined with magnetic resonance imaging (MRI) in assessment of LV and RV dysfunction accurately.[7,13−15] Real time three-dimensional (3D) echocardiography has become a convenient and reliable technique to assess ventricular volume and systolic function, but there are limited data on assessing RV and LV function on 2D and 3D transthoracic echocardiography (TTE) in patients with repaired TOF. Li et al. demonstrated that adverse 3D LV mechanics as characterized by impaired global and regional 3D systolic strain, mechanical dyssynchrony, and reduced twist is related to reduced septal curvature in repaired TOF patients.[9] Nakmura et al. reported that free wall longitudinal strain was significantly reduced despite preserved LVEF in patients with repaired TOF undergoing 2D and 3D TTE.[8] The feasibility of combined 2D and 3D TTE in patients with repaired TOF requires further evaluation. The present prospective study assessed biventricular performance in asymptomatic adolescents with repaired TOF using both 2D speckle tracking and real time 3D echocardiography.

2. Methods

2.1. Study population

This prospective study consisted of 31 consecutive asymptomatic Taiwanese patients with repaired TOF who were followed up at the department of Pediatrics, Kaohsiung Veterans General Hospital (KVGH), Taiwan, from August 2012 to December 2016. The mean age at surgery was 3 years. The mean postoperative follow-up duration was 12.8 years. All patients were in New York Heart Association (NYHA) class 1. Exclusion criteria were residual intracardiac shunts, severe tricuspid regurgitation, significant RV outflow tract obstruction (>30 mmHg), known or detected arrhythmia, history of cardiovascular medication, a lack of informed consent, and an inability to cooperate. Thirty two age- and sex-matched healthy Taiwanese controls were recruited. These control subjects were seen at the outpatient clinic for nonspecific chest pain and functional murmur for which no cardiac abnormalities were identifiable. All subjects underwent echocardiography, 12-lead electrocardiogram, exercise test, and blood sampling for brain natriuretic peptide (BNP) measurement. The study protocol was approved by KVGH Institutional Review Board for human subjects (VGHKS 14 − CT 2−07) and informed written consent was obtained from the subject or guardian.

2.2. Echocardiographic equipment and parameters

Echocardiography was performed using the Acuson SC2000 system (Siemens Medical Solutions USA, Inc., Mountain View, CA). During echocardiography, the subjects were at rest in the left lateral decubitus position. A comprehensive study including M-mode, color, 2D, and 3D echocardiography was performed. For speckle tracking analysis, two-dimensional grayscale images were obtained for the subjects using the apical four-chamber view at frame rates of 60−90 frames/sec. Further analysis was conducted with syngo Vector Velocity Imaging (Siemens Medical Solutions USA, Inc, Mountain View, CA). The speckle-tracking analysis was performed separately for the right and left ventricle and consisted of marking the endocardium in the end-systolic frame. The adequacy of speckle-tracking was visually checked and manually adjusted as required. This enables calculation of longitudinal strain and strain rate if performed in the apical view (Fig. 1).

2.3. Real time 3D echocardiographic image acquisition

Real time 3D echocardiographic images were obtained from the apical window with subjects during end-expiratory breath-hold. LV and RV full-volume real time 3D echocardiographic images were acquired in a single beat using the 4Z1c matrix-array transducer (frequency bandwidth, 1.5−3.5 MHz; maximum depth, 30 cm; maximum field of view, $90^0 \times 90^0$). For the RV, the probe position was adjusted for optimal simultaneous visualization of the tricuspid valve, cardiac apex, infundibulum, and RV outflow tract. Analyses were performed using the 3D analysis software provided on the echocardiographic system. Analysis of the 3D images was performed with the embedded LV analysis program of the system using an autocontouring algorithm and, if needed,

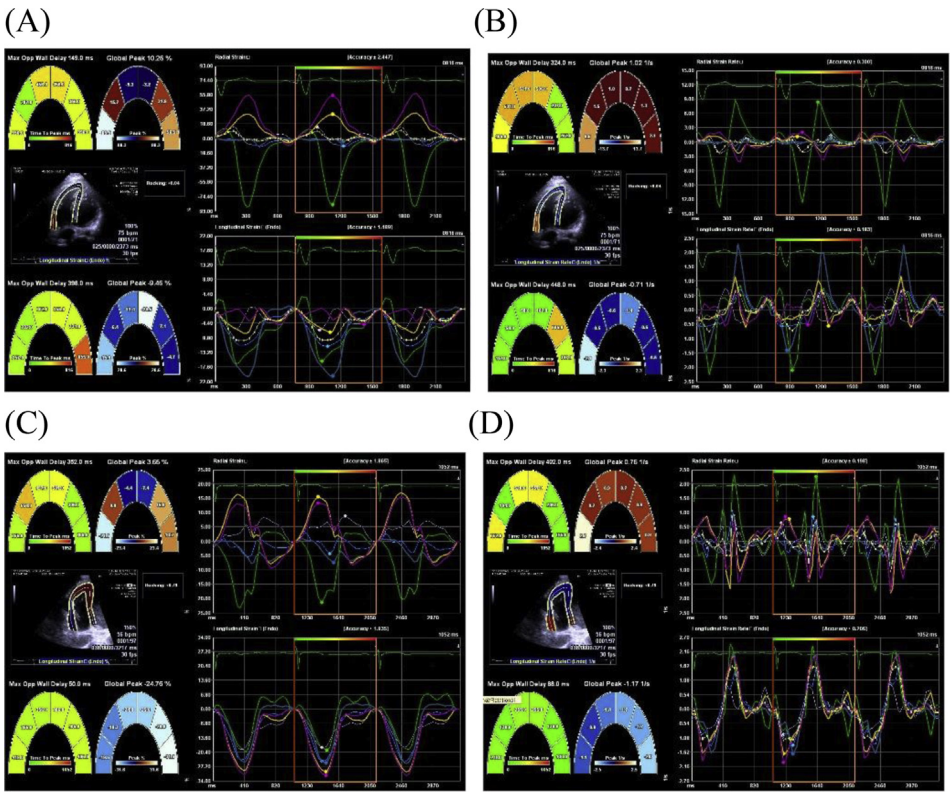

Fig. 1. Longitudinal strain (A)/strain rate (B) at apical view in a patient with repaired tetralogy of Fallot and strain (C)/strain rate (D) in a normal control.

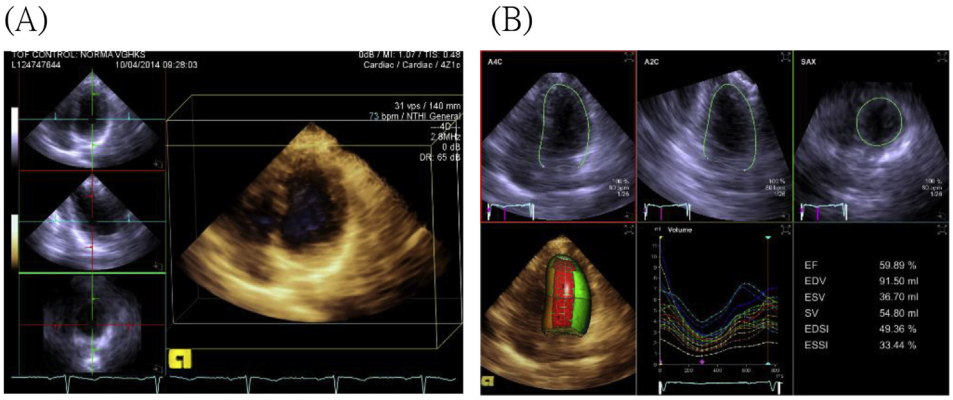

Fig. 2. The stepwise process of left ventricle (LV) reconstruction by 3D echocardiography. (A) Real time 3D echocardiographic images are reviewed in four planes (short-axis and apical two-chamber, three-chamber, and four-chamber views), and brightness and contrast are optimized. (B) LV endocardial border is automatically demonstrated (green line) by the LV analysis program when the "contour revision" is selected (auto-contouring algorithm). The endocardial border is optimized with additional manual correction if needed. LV volume is calculated and displayed.

manually corrected after a review of the traced border (Fig. 2). Full-volume 3D echocardiographic RV data sets were imported into the on-cart RV Analysis application. Manual adjustment of the RV data set was required to ensure the correct orientation of four-chamber, sagittal, and coronal slices; maximize the RV cavity area; identify the most apical RV view on visual assessment of the four-chamber window; and allow the identification of cardiac landmarks. Endocardial RV borders were traced at end-diastole and end-systole in four-chamber, basal sagittal, and coronal views. Trabeculae were included in the blood pool volume. Automated volumetric reconstruction was accepted only once the semiautomated endocardial border tracking was visually satisfactory and represented meaningful RV shapes in all views (Fig. 3).

The software-derived functional parameters LV end-diastolic volume index (LVEDVI), LV end-systolic volume index (LVESVI), LV stroke volume index (LVSVI) and LV ejection fraction (LVEF) were measured. In the same way, RV end-diastolic volume index (RVEDVI), RV end-systolic volume index (RVESVI), RV stroke volume index (RVSVI) and RVEF were measured. Cardiac index was measured using the following formula: LVSVI × heart rate at the examination. The pulmonary regurgitation fraction (PRF) was calculated using the following formula: (RVSVI−LVSVI)/RVSVI.[8]

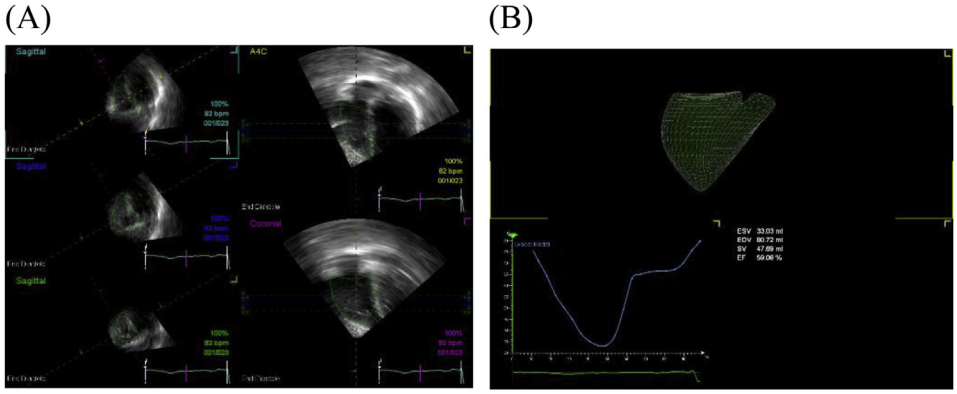

Fig. 3. The stepwise process of right ventricle (RV) reconstruction by 3D echocardiography. (A) Having traced endocardial borders in three orthogonal views, the border tracking results are displayed for inspection. Note how the purple guideline (indicated by the purple asterisk) bisects the tricuspid valve and RV outflow tract in the short-axis views. This corresponds to the coronal RV reconstruction (highlighted), with clearly delineated RV inflow and outflow portions. (B) RV volume is calculated and displayed.

2.4. BNP measurement

Blood was collected into tubes containing EDTA and centrifuged for assay. BNP was measured with a commercial ELISA kit.

2.5. Exercise stress test

All the subjects underwent exercise stress test by treadmill with standard Bruce protocol. The test was terminated if one of the following endpoints was reached: target HR, severe fatigue, severe dyspnea, severe ventricular arrhythmias. The following functional indexes were assessed at peak effort: maximal heart rate, maximal systolic blood pressure, peak oxygen consumption (VO2), and time duration of the exercise.

2.6. Statistical analysis

All data are presented as mean ± SD. Comparisons between groups were made using Student's *t*-test, Mann Whitney U test, or non-parametric tests depending on data distribution. Similarly, associations among variables were explored using the Spearman rank correlation coefficient or simple linear regression, as appropriate. A receiver operating characteristics (ROC) curve was generated and the area under the curve (AUC) was calculated to evaluate the specificity and sensitivity for dichotomization of QRS duration. Intra-observer and inter-observer variability was assessed in 10 patients with repaired TOF and 10 normal control subjects. Inter-observer and intra-observer variability of echocardiographic parameters was evaluated using the intraclass correlation coefficient (ICC). Data were analyzed using SPSS version 21 (SPSS, Chicago, IL, USA). $p < 0.05$ was considered statistically significant.

3. Results

The demographic and clinical data of the subjects are presented in Table 1. Age, sex, weight, and body mass index were not significantly different between two groups. There was significant difference between the two groups in terms of height ($p < 0.05$), BNP ($p < 0.01$), peak VO2 ($p < 0.05$), RV fractional area change ($p < 0.05$), tricuspid annular plane systolic excursion (TAPSE) ($p < 0.05$), and QRS duration ($p < 0.01$).

Table 1
Baseline characteristics of TOF patients and normal controls.

Variable	TOF	Control	*p*
	n = 31	n = 32	
Age (years)	16.1 ± 6.1	16.6 ± 5.1	0.657
Male/female	22/9	23/9	0.936
Height (cm)	151.7 ± 26.0	173.7 ± 52.4	0.040
Weight (kg)	48.4 ± 15.4	51.4 ± 10.7	0.368
BNP (pg/ml)	31.8 ± 21.4	14.1 ± 12.4	0.006
Peak VO2 (ml/kg/min)	8.4 ± 1.7	9.9 ± 1.6	0.015
RV fractional area of change (%)	40.2 ± 9.4	46.5 ± 9.4	0.026
TAPSE (mm)	14.2 ± 4.8	20.6 ± 4.2	0.016
Heart rate (beats/min)	72.8 ± 14.9	73.2 ± 21.6	0.934
QRS (ms)	126 ± 30	82 ± 9	0.001

BNP = brain natriuretic peptide; VO2 = oxygen consumption; TAPSE = tricuspid annular plane systolic excursion; TOF = tetralogy of Fallot.

3.1. Comparison of strain and strain rate between normal and repaired TOF groups

The LV and RV regional and global longitudinal strain (GLS) for the control and repaired TOF groups are shown in Table 2. Compared to normal controls, patients with repaired TOF had significantly reduced longitudinal strain of middle septal, apical septal, apical lateral segments in LV and all segments in RV. In the patients with repaired TOF, there was a progressive decrease of lateral RV regional strain from base to apex, with the basal segments significantly higher than the apical segments ($p < 0.05$). GLS in both LV and RV were significantly impaired in patients with repaired TOF compared with normal controls. In addition, there was a significant correlation of LV-GLS and RV-GLS (r = 0.456, $p = 0.01$) in patients with repaired TOF. The LV and RV regional and

Table 2
Peak longitudinal strain.

	TOF	Control	p
LV			
Basal septal (%)	−12.53 ± 13.99	−17.64 ± 7.49	0.518
Middle septal (%)	−11.50 ± 12.40	−18.88 ± 6.75	0.005
Apical septal (%)	−9.03 ± 17.07	−23.94 ± 15.36	0.001
Apical lateral (%)	−12.32 ± 16.98	−23.10 ± 8.25	0.002
Middle lateral (%)	−16.56 ± 13.84	−17.25 ± 8.03	0.810
Basal lateral (%)	−16.19 ± 12.92	−18.82 ± 7.89	0.331
Global (%)	−12.82 ± 11.13	−19.75 ± 4.95	0.001
RV			
Basal lateral (%)	−16.04 ± 14.41	−29.38 ± 14.43	0.001
Middle lateral (%)	−12.16 ± 10.43	−21.41 ± 14.27	0.005
Apical lateral (%)	−10.14 ± 14.99	−20.46 ± 15.71	0.010
Apical septal (%)	−11.40 ± 15.98	−20.34 ± 12.12	0.015
Middle septal (%)	−12.21 ± 9.86	−21.35 ± 10.93	0.001
Basal septal (%)	−13.43 ± 12.65	−24.11 ± 12.29	0.001
Global (%)	−12.32 ± 11.03	−22.98 ± 6.89	0.000

LV = left ventricle; RV = right ventricle; TOF = tetralogy of Fallot.

Table 3
Peak longitudinal strain rate.

	TOF	Control	p
LV			
Basal septal (1/s)	−1.12 ± 0.54	−1.07 ± 0.53	0.676
Middle septal (1/s)	−0.97 ± 0.27	−1.08 ± 0.42	0.224
Apical septal (1/s)	−1.22 ± 0.56	−1.81 ± 0.57	0.000
Apical lateral (1/s)	−1.21 ± 0.50	−1.50 ± 0.63	0.050
Middle lateral (1/s)	−1.22 ± 0.56	−1.01 ± 0.36	0.173
Basal lateral (1/s)	−1.28 ± 0.51	−1.28 ± 0.54	0.985
Global (1/s)	−0.97 ± 0.31	−1.16 ± 0.32	0.017
RV			
Basal lateral (1/s)	−1.26 ± 0.51	−2.33 ± 1.10	0.000
Middle lateral (1/s)	−0.95 ± 0.38	−1.76 ± 0.67	0.000
Apical lateral (1/s)	−0.93 ± 0.47	−1.71 ± 0.98	0.000
Apical septal (1/s)	−1.11 ± 0.37	−1.62 ± 0.80	0.012
Middle septal (1/s)	−0.94 ± 0.33	−1.59 ± 0.86	0.000
Basal septal (1/s)	−1.10 ± 0.47	−1.89 ± 1.25	0.000
Global (1/s)	−0.87 ± 0.31	−1.60 ± 0.64	0.000

LV = left ventricle; RV = right ventricle; TOF = tetralogy of Fallot.

global longitudinal strain rate (GLSR) for the control and repaired TOF groups are shown in Table 3. Compared to normal controls, patients with repaired TOF had significantly reduced longitudinal strain rate of septal, apical septal, apical lateral segments in LV and all segments in RV. LV-GLSR and RV-GLSR were significantly impaired in patients with repaired TOF compared with normal controls.

Time to peak longitudinal strain in both groups is shown in Table 4. Compared to the normal controls, patients with repaired TOF had significantly longer time to peak longitudinal strain in terms of basal lateral, apical lateral, basal septal, and apical septal segments in RV. In addition, there was a significant correlation of LV- and RV-global time to peak longitudinal strain ($r = 0.484$, $p < 0.01$) in patients with repaired TOF. Time to peak longitudinal strain rate in both groups is shown in Table 5 separately. There is no significant difference in both groups in terms of time to peak longitudinal regional and global strain rate.

Table 4
Time to peak longitudinal strain.

	TOF	Control	p
LV			
Basal septal (ms)	357.74 ± 155.15	318.47 ± 82.69	0.213
Middle septal (ms)	360.48 ± 165.50	316.22 ± 74.30	0.299
Apical septal (ms)	318.65 ± 118.96	307.31 ± 73.99	0.611
Apical lateral (ms)	329.45 ± 96.56	296.34 ± 65.56	0.115
Middle lateral (ms)	335.19 ± 98.28	351.84 ± 102.46	0.513
Basal lateral (ms)	344.42 ± 103.78	325.91 ± 79.50	0.429
Global (ms)	358.13 ± 166.52	314.13 ± 74.56	0.179
RV			
Basal lateral (ms)	376.94 ± 109.94	314.03 ± 65.51	0.021
Middle lateral (ms)	353.13 ± 130.02	319.00 ± 96.57	0.240
Apical lateral (ms)	348.39 ± 120.32	298.81 ± 76.23	0.055
Apical septal (ms)	365.35 ± 103.77	310.53 ± 80.41	0.022
Middle septal (ms)	335.13 ± 85.56	316.50 ± 74.68	0.360
Basal septal (ms)	399.52 ± 170.34	306.91 ± 80.14	0.021
Global (ms)	356.77 ± 129.73	305.81 ± 50.47	0.099

LV = left ventricle; RV = right ventricle; TOF = tetralogy of Fallot.

Table 5
Time to peak longitudinal strain rate.

	TOF	Control	p
LV			
Basal septal (ms)	150.89 ± 73.43	137.89 ± 66.52	0.464
Middle septal (ms)	129.81 ± 74.65	131.47 ± 61.39	0.923
Apical septal (ms)	143.16 ± 83.69	145.86 ± 58.05	0.882
Apical lateral (ms)	154.47 ± 97.21	136.56 ± 52.78	0.716
Middle lateral (ms)	180.52 ± 93.05	163.09 ± 81.16	0.431
Basal lateral (ms)	167.19 ± 88.22	152.54 ± 91.30	0.520
Global (ms)	133.68 ± 59.60	141.76 ± 53.66	0.573
RV			
Basal lateral (ms)	217.03 ± 146.18	207.28 ± 166.75	0.806
Middle lateral (ms)	252.58 ± 242.02	202.41 ± 169.90	0.343
Apical lateral (ms)	296.23 ± 307.92	202.41 ± 166.90	0.842
Apical septal (ms)	312.94 ± 281.57	238.69 ± 225.58	0.635
Middle septal (ms)	236.74 ± 196.08	170.44 ± 112.87	0.165
Basal septal (ms)	259.68 ± 240.54	193.41 ± 164.24	0.205
Global (ms)	225.45 ± 222.41	184.88 ± 154.07	0.405

LV = left ventricle; RV = right ventricle; TOF = tetralogy of Fallot.

Table 6
Three dimensional echocardiographic RV/LV volume and function.

	TOF	Control	p
LVEDVI (ml/m^2)	53.71 ± 13.88	57.22 ± 10.96	0.286
LVESVI (ml/m^2)	39.18 ± 71.01	24.89 ± 6.81	0.285
LVEF (%)	48.30 ± 14.65	51.46 ± 18.26	0.453
LVSVI (ml/m^2)	26.91 ± 11.19	32.35 ± 7.21	0.031
RVEDVI (ml/m^2)	96.92 ± 28.82	52.35 ± 10.99	0.000
RVESVI (ml/m^2)	45.72 ± 20.36	25.75 ± 6.15	0.000
RVEF (%)	52.71 ± 9.67	50.33 ± 8.82	0.343
RVSVI (ml/m^2)	50.78 ± 15.37	26.60 ± 8.02	0.000
Cardiac index (L · beats^{-1} · min^{-1} · m^{-2})	2.02 ± 0.94	2.28 ± 0.81	0.329
PRF	0.39 ± 0.28	−0.02 ± 0.06	0.000
RV/LV EDVI ratio	1.87 ± 0.58	0.93 ± 0.19	0.000

EF = ejection fraction; EDVI = end-diastolic volume index; ESVI = end-systolic volume index; LV = left ventricle; PRF = pulmonary regurgitation fraction; RV = right ventricle; SVI = stroke volume index; TOF = tetralogy of Fallot.

3.2. Comparison of 3D echocardiographic volume data between normal and repaired TOF groups

3D echocardiographic volume data in both groups are shown in Table 6. Compared to normal controls, patients with repaired TOF had lower LVSVI (26.91 ± 11.19 vs 32.35 ± 7.21 ml/m^2, $p < 0.05$), but higher RVEDVI (96.92 ± 28.82 vs 52.35 ± 10.99 ml/m^2, $p < 0.01$), RVESVI (45.72 ± 20.36 vs 25.75 ± 6.15 ml/m^2, $p < 0.01$), RVSVI (50.78 ± 15.37 vs 26.60 ± 8.02 ml/m^2, $p < 0.01$), PRF (0.39 ± 0.28 vs −0.02 ± 0.06, $p < 0.01$), and RV/LV EDVI ratio (1.87 ± 0.58 vs 0.93 ± 0.19, $p < 0.01$). There was no significant difference between two groups in terms of LVEDVI, LVESVI, LVEF, RVEF, and cardiac index.

3.3. Comparison of strain and strain rate between repaired TOF subgroups (QRS > 140 ms or ≤ 140 ms)

Patients with repaired TOF were divided in two subgroups (QRS > 140 ms or ≤ 140 ms) based on the ROC curve analysis (sensitivity 76.9%, specificity 70.6%, AUC = 0.715, $p < 0.05$). Patients with QRS ≤ 140 ms had higher longitudinal strain in lateral basal and middle segments in RV than those with QRS > 140 ms (Table 7). There was no significant difference of LV strain between patients with QRS > 140 ms and those with QRS ≤ 140 ms (data not shown). There was a significant correlation of QRS duration and RV middle lateral strain ($p < 0.01$) (Table 8). There was a significant correlation of QRS duration and strain rate in terms of RV basal septal ($p < 0.05$), RV middle lateral ($p < 0.001$), RV basal lateral ($p < 0.05$), RV global ($p < 0.05$), LV apical lateral ($p < 0.05$), and LV global ($p < 0.05$) strain rate (Table 8).

3.4. Inter-observer and intra-observer variability of 2D and 3D echocardiography

The inter-observer ICC was 0.95 for strain and 0.94 for strain rate. The intra-observer ICC was 0.96 and 0.95 for strain and strain rate, respectively. The inter-observer ICC for 3D echocardiography was 0.90, while the intra-observer ICC for 3D echocardiography was 0.92.

Table 7
Longitudinal peak strain in TOF patients with QRS ≤ 140 ms and QRS > 140 ms.

	≤140 ms (n = 15)	>140 ms (n = 16)	p
LV			
Basal septal (%)	−17.21 ± 6.85	−8.14 ± 17.47	0.338
Middle septal (%)	−14.15 ± 8.92	−9.03 ± 14.82	0.257
Apical septal (%)	−13.54 ± 11.93	−4.79 ± 20.26	0.379
Apical lateral (%)	−17.25 ± 10.11	−7.71 ± 20.83	0.119
Middle lateral (%)	−18.97 ± 5.56	−14.31 ± 18.52	0.357
Basal lateral (%)	−17.36 ± 4.85	−15.09 ± 17.59	0.599
Global (%)	−15.88 ± 4.37	−9.96 ± 14.55	0.572
RV			
Basal lateral (%)	−21.58 ± 9.06	−10.84 ± 16.71	0.036
Middle lateral (%)	−17.00 ± 4.39	−7.63 ± 12.43	0.049
Apical lateral (%)	−11.92 ± 15.51	−8.48 ± 14.79	0.532
Apical septal (%)	−11.96 ± 17.49	−10.87 ± 15.00	0.853
Middle septal (%)	−15.01 ± 6.11	−9.59 ± 12.02	0.128
Basal septal (%)	−18.77 ± 6.51	−8.42 ± 15.00	0.066
Global (%)	−15.95 ± 7.27	−8.91 ± 12.98	0.078

LV = left ventricle; RV = right ventricle; TOF = tetralogy of Fallot.

Table 8
Correlation of QRS duration with strain and strain rate in patients with repaired TOF.

	QRS duration (ms)		
	R^2	β	p
RV strain			
Basal septal (%)	0.144	−0.380	0.051
Middle septal (%)	0.067	−0.259	0.192
Apical septal (%)	0.021	0.145	0.472
Apical lateral (%)	0.002	0.039	0.845
Middle lateral (%)	0.253	−0.503	0.008
Basal lateral (%)	0.068	−0.262	0.188
Global (%)	0.060	−0.244	0.219
RV strain rate			
Basal septal (1/s)	0.190	−0.436	0.023
Middle septal (1/s)	0.101	−0.317	0.107
Apical septal (1/s)	0.127	−0.356	0.069
Apical lateral (1/s)	0.108	−0.328	0.094
Middle lateral (1/s)	0.471	−0.687	<0.001
Basal lateral (1/s)	0.194	−0.441	0.021
Global (1/s)	0.187	−0.433	0.024
LV strain			
Basal septal (%)	0.089	−0.299	0.108
Middle septal (%)	0.023	−0.152	0.423
Apical septal (%)	0.065	−0.255	0.173
Apical lateral (%)	0.095	−0.308	0.098
Middle lateral (%)	0.022	−0.149	0.432
Basal lateral (%)	0.021	−0.144	0.448
Global (%)	0.098	0.313	0.092
LV strain rate			
Basal septal (1/s)	0.028	−0.168	0.375
Middle septal (1/s)	0059	−0.244	0.195
Apical septal (1/s)	0.088	−0.297	0.111
Apical lateral (1/s)	0.206	−0.454	0.012
Middle lateral (1/s)	0.045	−0.211	0.263
Basal lateral (1/s)	0.009	0.094	0.623
Global (1/s)	0.148	−0.385	0.036

LV = left ventricle; RV = right ventricle; TOF = tetralogy of Fallot.

4. Discussion

Our study demonstrated that asymptomatic patients with repaired TOF had decreased biventricular strain and strain rate than normal controls. The 3D echocardiographic volume analysis further showed that there was significant RV dysfunction in patients with repaired TOF. Compatible with previous studies,[4,8,15] our results suggested that both 2D STE and 3D echocardiography may be useful in the serial evaluation of ventricular function in patients with repaired TOF.

Previous studies have established RV dilatation and reduced RV function in patients late after repair of TOF.[3–5] A correlation between LV and RV systolic dysfunction on MRI has been reported, suggesting an unfavorable ventricular interaction.[6] In agreement with a previous study that used MRI,[6] there was a significant correlation between LV- and RV-GLS (or global time to peak longitudinal strain) in patients with repaired TOF in our study. Assessment of ventricular function by MRI is based on

ejection fraction (indirect measurement), but 2D speckle tacking longitudinal strain quantifies myocardial deformation directly.[4,15] In terms of regional strain/strain rate change in patients with repaired TOF, both free wall and septum of RV were entirely affected, and there is a very striking reduction in regional myocardial strain from RV basal to apical segments. A similar finding was initially demonstrated in patients with pulmonary arterial hypertension (PAH).[16,17] Dambrauskaite et al.[16] showed that apical RV longitudinal strain was more significantly decreased compared with other RV segments in patients with PAH, using tissue Doppler derived measurements. In Sachdev et al.' data regarding patients with PAH, apical RV strain values were much lower than basal and mid RV values.[17] Dragulescu A et al. first documented the decrease of RV apical function in patients with repaired TOF.[18] However, it is unclear why RV apical function is more severely affected. One important factor might be regional myocardial geometry change related to dilatation of RV. RV shape changes in patients with repaired TOF have previously been reported.[19,20] MRI analysis of TOF patients in Bodhey et al.'s study showed that the adaptive response depended majorly on the RV apical trabecular component for RV dilation due to PR.[19] In addition, Sheehan et al. demonstrated that the RV apex had a more dilated and round shape in patients with repaired TOF compared to normal controls, and speculated that the larger regional RV radii of curvature at the apex might make patients with repaired TOF have a higher regional wall stress, which results in more significantly reduced regional myocardial deformation.[20] In contrast to the decrease in apical function, the basal longitudinal function in patients with repaired TOF is relatively preserved. This can partly explain why the RV can maintain the increased output despite the decreased apical function. Further longitudinal study is required to investigate the changes in regional RV myocardial function and provide data about when to perform pulmonary valve replacement (PVR) for patients with repaired TOF.

In contrast to the decreased strain/strain rate of all RV segments in this series, the LV strain/strain rate decreased significantly in part, mainly in the apical segment. However, the mechanism causing the partial decrease of LV strain/strain rate requires elucidation. Factors for LV dysfunction in patients with repaired TOF included PR, RV dilatation, paradoxical IVS motion, duration of preoperative hypoxia, myocardial fibrosis, techniques for surgical repair, electrical factor (prolonged QRS duration), etc.[15,21] van der Hulst et al. demonstrated the significant relationship of RV and LV global strains, indicating the presence of ventricular–ventricular interactions.[22] Their results[22] also revealed a homogenous decrease of longitudinal RV strain in all segments, whereas LV longitudinal strain reduced significantly only at the mid and apical levels. It is an interesting issue about the earlier impairment of LV strain in apical segment than in basal segment. Both Bodhey et al.'s[19] and Sheehan et al.'s[20] studies suggest the RV apical adaption to volume overload may induce change in the apical LV geometry that could result in apical LV dysfunction. According to these previous reports,[19,20] it is reasonable to speculate that LV longitudinal strain at the apex may decrease at an earlier stage than that at the basal segment. Our results suggest abnormal ventricular interaction may be an important factor for reduced LV strain and are similar to those of Van der Hulst et al.[22]

Our analysis showed that the regional RV strain are significantly reduced in patients with QRS duration > 140 ms than those with QRS $\leq$ 140 ms. The correlation of QRS duration and RV strain showed the significant correlation in RV middle lateral area. On the other hand, there was no significant difference of LV strain between patients with QRS > 140 ms and those with QRS $\leq$ 140 ms. Further analysis of QRS duration and LV regional and global strain also showed no significant relationship. QRS prolongation in patients with repaired TOF are related to RV dilatation, wall motion abnormalities, and life-threatening arrhythmias.[23] Abd El Rahman et al. further reported QRS prolongation associated with right bundle branch morphology is not sensitive for the detection of LV asynchrony in patients after TOF repair.[21] These previous findings may partially explain the significant effect of QRS prolongation on RV strain, but not on LV strain. However, our results showed there was a significant correlation of QRS duration and strain rate in terms of RV basal septal, RV middle lateral, RV basal lateral, RV global, LV apical lateral, and LV global segments. It may imply prolonged QRS duration is associated with both certain regional and global abnormal biventricular performance. Strain rate is less influenced by loading conditions than strain, so this may elucidate why there is more correlation of QRS duration with strain rate than with strain. The effect of prolonged QRS duration on LV function requires further evaluation, especially about the issue of cardiac resynchronization therapy on improving ventricular function.[24]

Our patients with repaired TOF had high BNP levels, significantly exceeding those in healthy controls; however, most of them did not exceed the accepted normal value. Heng et al. reported that BNP level $\geq$52 pg/mL is associated with a fivefold increased risk of death in patients with repaired TOF.[25] Hirono et al. demonstrated that NT-pro-BNP was the strongest predictor of PVR in patients with surgically corrected TOF.[26] Ishii et al.'s findings showed that greater increases of BNP after exercise are associated with impaired RV contractile reserve in patients with TOF with various degrees of PR.[27] Further studies are required to elucidate the role of BNP in patients with repaired TOF.

We need to mention several limitations. Only 6 segments of LV, not all 16 segments, were analyzed for the longitudinal strain and strain rate in apical view. LV global longitudinal strain and strain rate were not actual average values, but represented only estimated average values. There is no data about circumferential and radial strain/strain rate. MRI was not used for validation of 3D volume analysis. The effect of prenatal[28] or postoperative[29] factors on myocardial function was not included in the analysis. This is a single-center investigation with limited number of patients. The relationship of 2D STE and 3D echocardiography requires further evaluation.

In conclusion, our results suggest asymptomatic adolescents with repaired TOF had abnormal biventricular myocardial performance, as demonstrated by combined speckle-tracking and 3D echocardiography. The implications of these

findings for management of adolescents late after repaired TOF remain to be determined.

Acknowledgments

Part of this research was supported by the Kaohsiung Veterans General Hospital (VGHUST104-G7-7-3, VGHK S105-106, VGHUST105-G3-1-3, and VGHKS106-120) and the Ministry of Science and Technology, R.O.C. (MOST 104-2314-B-075B-007).

References

1. Wu MH, Chen HC, Lu CW, Wang JK, Huang SC, Huang SK. Prevalence of congenital heart disease at live birth in Taiwan. *J Pediatr* 2010;**156**:782−5.
2. Murphy JG, Gersh BJ, Mair DD, Fuster V, McGoon MD, Ilstrup DM, et al. Long-term outcome in patients undergoing surgical repair of tetralogy of Fallot. *N Engl J Med* 1993;**329**:593−9.
3. Valente AM, Gauvreau K, Assenza GE, Babu-Narayan SV, Schreier J, Gatzoulis MA, et al. Contemporary predictors of death and sustained ventricular tachycardia in patients with repaired tetralogy of Fallot enrolled in the INDICATOR cohort. *Heart* 2014;**100**:247−53.
4. Kempny A, Diller GP, Orwat S, Kaleschke G, Kerckhoff G, Bunck ACh, et al. Right ventricular-left ventricular interaction in adults with Tetralogy of Fallot: a combined cardiac magnetic resonance and echocardiographic speckle tracking study. *Int J Cardiol* 2012;**154**:259−64.
5. Rowe SA, Zahka KG, Manolio TA, Horneffer PJ, Kidd L. Lung function and pulmonary regurgitation limit exercise capacity in postoperative tetralogy of Fallot. *J Am Coll Cardiol* 1991;**17**:461−6.
6. Davlouros PA, Kilner PJ, Hornung TS, Li W, Francis JM, Moon JC, et al. Right ventricular function in adults with repaired tetralogy of Fallot assessed with cardiovascular magnetic resonance imaging: detrimental role of right ventricular outflow aneurysms or akinesia and adverse right-to-left ventricular interaction. *J Am Coll Cardiol* 2002;**40**:2044−52.
7. Diller GP, Kempny A, Liodakis E, Alonso-Gonzalez R, Inuzuka R, Uebing A, et al. Left ventricular longitudinal function predicts life-threatening ventricular arrhythmia and death in adults with repaired tetralogy of Fallot. *Circulation* 2012;**125**:2440−6.
8. Nakamura A, Horigome H, Seo Y, Ishizu T, Sumazaki R. Right ventricular remodeling due to pulmonary regurgitation is associated with reduced left ventricular free wall strain in surgically repaired tetralogy of Fallot. *Circ J* 2014;**78**:1960−6.
9. Li SN, Yu W, Lai CT, Wong SJ, Cheung YF. Left ventricular mechanics in repaired tetralogy of Fallot with and without pulmonary valve replacement: analysis by three-dimensional speckle tracking echocardiography. *PLoS One* 2013;**8**:e78826.
10. Anderson RH, Ho SY, Redmann K, Sanchez-Quintana D, Lunkenheimer PP. The anatomical arrangement of the myocardial cells making up the ventricular mass. *Eur J Cardiothorac Surg* 2005;**28**:517−25.
11. Helbing WA, Roest AA, Niezen RA, Vliegen HW, Hazekamp MG, Ottenkamp J, et al. ECG predictors of ventricular arrhythmias and biventricular size and wall mass in tetralogy of Fallot with pulmonary regurgitation. *Heart* 2002;**88**:515−9.
12. Weyman AE, Wann S, Feigenbaum H, Dillon JC. Mechanism of abnormal septal motion in patients with right ventricular volume overload: a cross-sectional echocardiographic study. *Circulation* 1976;**54**:179−86.
13. Friedberg MK, Fernandes FP, Roche SL, Grosse-Wortmann L, Manlhiot C, Fackoury C, et al. Impaired right and left ventricular diastolic myocardial mechanics and filling in asymptomatic children and adolescents after repair of tetralogy of Fallot. *Eur Heart J Cardiovasc Imaging* 2012;**13**:905−13.
14. Fernandes FP, Manlhiot C, Roche SL, Grosse-Wortmann L, Slorach C, McCrindle BW, et al. Impaired left ventricular myocardial mechanics and their relation to pulmonary regurgitation, right ventricular enlargement and exercise capacity in asymptomatic children after repair of tetralogy of Fallot. *J Am Soc Echocardiogr* 2012;**25**:494−503.
15. Li Y, Xie M, Wang X, Lu Q, Zhang L, Ren P. Impaired right and left ventricular function in asymptomatic children with repaired tetralogy of fallot by two-dimensional speckle tracking echocardiography study. *Echocardiography* 2015;**32**:135−43.
16. Dambrauskaite V, Delcroix M, Claus P, Herbots L, D'hooge J, Bijnens B, et al. Regional right ventricular dysfunction in chronic pulmonary hypertension. *J Am Soc Echocardiogr* 2007;**20**:1172−80.
17. Sachdev A, Villarraga HR, Frantz RP, McGoon MD, Hsiao JF, Maalouf JF, et al. Right ventricular strain for prediction of survival in patients with pulmonary arterial hypertension. *Chest* 2011;**139**:1299−309.
18. Dragulescu A, Grosse-Wortmann L, Redington A, Friedberg MK, Mertens L. Differential effect of right ventricular dilatation on myocardial deformation in patients with atrial septal defects and patients after tetralogy of Fallot repair. *Int J Cardiol* 2013;**168**:803−10.
19. Bodhey NK, Beerbaum P, Sarikouch S, Kropf S, Lange P, Berger F, et al. Functional analysis of the components of the right ventricle in the setting of tetralogy of Fallot. *Circ Cardiovasc Imaging* 2008;**1**:141−7.
20. Sheehan FH, Ge S, Vick III GW, Urnes K, Kerwin WS, Bolson EL, et al. Three-dimensional shape analysis of right ventricular remodeling in repaired tetralogy of Fallot. *Am J Cardiol* 2008;**101**:107−13.
21. Abd El Rahman MY, Hui W, Yigitbasi M, Dsebissowa F, Schubert S, Hetzer R, et al. Detection of left ventricular asynchrony in patients with right bundle branch block after repair of tetralogy of Fallot using tissue-Doppler imaging-derived strain. *J Am Coll Cardiol* 2005;**45**:915−21.
22. van der Hulst AE, Delgado V, Holman ER, Kroft LJ, de Roos A, Hazekamp MG, et al. Relation of left ventricular twist and global strain with right ventricular dysfunction in patients after operative "correction"of tetralogy of Fallot. *Am J Cardiol* 2010;**106**:723−9.
23. Gatzoulis MA, Till JA, Somerville J, Redington AN. Mechanoelectrical interaction in tetralogy of Fallot. QRS prolongation relates to right ventricular size and predicts malignant ventricular arrhythmias and sudden death. *Circulation* 1995;**92**:231−7.
24. Merchant FM, Kella D, Book WM, Langberg JJ, Lloyd MS. Cardiac resynchronization therapy in adult patients with repaired tetralogy of fallot and left ventricular systolic dysfunction. *Pacing Clin Electrophysiol* 2014;**37**:321−8.
25. Heng EL, Bolger AP, Kempny A, Davlouros PA, Davidson S, Swan L, et al. Neurohormonal activation and its relation to outcomes late after repair of tetralogy of Fallot. *Heart* 2015;**101**:447−54.
26. Hirono K, Sekine M, Shiba N, Hayashi S, Nakaoka H, Ibuki K, et al. N-terminal pro-brain natriuretic peptide as a predictor of reoperation in children with surgically corrected tetralogy of Fallot. *Circ J* 2014;**78**:693−700.
27. Ishii H, Harada K, Toyono M, Tamura M, Takada G. Usefulness of exercise-induced changes in plasma levels of brain natriuretic peptide in predicting right ventricular contractile reserve after repair of tetralogy of Fallot. *Am J Cardiol* 2005;**95**:1338−43.
28. Hung JH, Lu JH, Weng ZC, Chen CY, Chao KC, Hung CY. Prenatal diagnosis of tetralogy of Fallot with pulmonary atresia. *J Chin Med Assoc* 2008;**71**:262−6.
29. Liang CM, Hwang B, Lu JH, Lee PC, Weng ZC, Ho TY, et al. Risk factors of prolonged postoperative pleural effusion after repair of tetralogy of Fallot. *J Chin Med Assoc* 2005;**68**:406−10.